6-inch uniform vertically-oriented graphene on soda-lime glass for photothermal applications

Haina Ci^{1,2}, Huaying Ren^{1,2}, Yue Qi^{1,2}, Xudong Chen¹, Zhaolong Chen¹, Jincan Zhang^{1,2}, Yanfeng Zhang^{1,3} (⋈), and Zhongfan Liu¹ (⋈)

Received: 13 June 2017 Revised: 21 August 2017 Accepted: 1 September 2017

© Tsinghua University Press and Springer-Verlag GmbH Germany 2017

KEYWORDS

vertically oriented graphene (VG), soda-lime glass, photothermal application, antireflective material

ABSTRACT

Vertically-oriented graphene (VG) has many advantages over flat lying graphene, including a large surface area, exposed sharp edges, and non-stacking three-dimensional geometry. Recently, VG nanosheets assembled on specific substrates have been used for applications in supersensitive gas sensors and high-performance energy storage devices. However, to realize these intriguing applications, the direct growth of high-quality VG on a functional substrate is highly desired. Herein, we report the direct synthesis of VG nanosheets on traditional soda-lime glass due to its low-cost, good transparency, and compatibility with many applications encountered in daily life. This synthesis was achieved by a direct-current plasma enhanced chemical vapor deposition (dc-PECVD) route at 580 °C, which is right below the softening point of the glass, and featured a scale-up size ~ 6 inches. Particularly, the fabricated VG nanosheets/glass hybrid materials at a transmittance range of 97%-34% exhibited excellent solarthermal performances, reflected by a 70%-130% increase in the surface temperature under simulated sunlight irradiation. We believe that this graphene glass hybrid material has great potential for use in future transparent "green-warmth" construction materials.

Graphene, consisting of sp²-bonded carbon atoms regularly packed into a two dimensional (2D) honeycomb structure, has attracted widespread attention owing to its excellent electrical, mechanical, optical, and thermal properties [1–4]. Glass is a commonly

used transparent, insulating, amorphous oxide with high surface hydrophilicity and low thermal conductivity. The combination of graphene with glass can improve the electrical and thermal properties of the glass while maintaining its transparency. Our group

Address correspondence to Zhongfan Liu, zfliu@pku.edu.cn; Yanfeng Zhang, yanfengzhang@pku.edu.cn



¹ Center for Nanochemistry (CNC), Beijing Science and Engineering Center for Nanocarbons, College of Chemistry and Molecular Engineering, Peking University, Beijing 100871, China

² Academy for Advanced Interdisciplinary Studies, Peking University, Beijing 100871, China

³ Department of Materials Science and Engineering, College of Engineering, Peking University, Beijing 100871, China

has developed several routes to directly grow 2D graphene on glass targeting different applications [5–9]. For example, atmospheric-pressure chemical vapor deposition (APCVD) growth of several-layer graphene films on quartz glass for high-performance touch panel applications, molten-state APCVD growth of 1–2 layers of graphene on molten-glass for cell culture, and low-pressure CVD (LPCVD) synthesis of thickness-controllable graphene on quartz glass for switchable window. These graphene syntheses were generally performed on high melting point quartz glass at a 1,000–1,100 °C growth temperature with a duration of several hours.

In addition to the conventional 2D graphene, vertically oriented graphene (VG) nanosheets, composed by mono- or few-layer graphene, have been synthesized via a plasma-enhanced chemical vapor deposition (PECVD) route on metal or dielectric substrates [10–16]. Many unique properties, including large amount of exposed edges, non-stacking geometry, and a large surface-to-volume ratio were obtained in these threedimensional (3D) graphene nanosheets. In particular, different applications similar to their 2D counterparts have been developed. The VG nanosheets synthesized on nickel substrates, Au electrodes, and silicon substrates by radio frequency (rf) PECVD, direct-current (dc)-PECVD, and micro-wave (mw) PECVD routes have been utilized as double-layer capacitors (DLCs), gas sensors, and electrochemical transducers, respectively [10–12]. A relatively high growth temperature (900– 1,200 °C), including the use of metal catalysts or metallic substrates were usually adopted as part of the synthetic strategy. Moreover, these applications mainly took advantage of the high surface-to-volume ratio and conductivity properties of the VG nanosheets.

Recently, VG nanosheets have also been synthesized on insulating glass substrates at relatively low temperatures between 500–900 °C, with the aid of either a metal catalyst layer or a copper-assisted remotecatalysis process via rf-PECVD [17, 18]. However, these conditions resulted in long growth time and small physical dimensions, which are not suitable for many applications. Moreover, glass with high melting points, like quartz, are very expensive. For a commercial low-cost float glass with a softening temperature of ~ 600 °C, the direct synthesis of high-quality, large-scale,

uniform, VG without introducing any metal catalyst remains a challenge.

Herein, we describe the development of a dc-PECVD fabrication route for the fast growth of large-scale uniform VG on common soda-lime glass, with a growth temperature right below the softening point of the glass substrates. 6-inch uniform VG nanosheet-glass hybrid materials were obtained within 10 min for growth at 580 °C, with a resulting transparency of over 75% at 550 nm. In addition, the internal mechanisms that dominate the vertical growth of graphene on glass were also determined through a systematical investigation of the growth process. Furthermore, the large-scale, uniform, VG nanosheet-glass was employed as a high-performance photothermal material by taking advantage of its unique sheet resistance vs. transparency. In this regard, the VG nanosheet-glass hybrid material may serve as a promising candidate for use in transparent solarthermal devices and green warmth construction materials.

The growth characteristics of graphene on glass in our experiments are summarized in Fig. 1(a). The dc-PECVD set-up is shown in Fig. S1 in the Electronic Supplementary Material (ESM). At the initial stage, the carbon precursor of CH₄ was dissociated into highly reactive species (CH_{xr} C₂H_{yr}, and atomic C and H) by direct current glow discharge [19, 20]. These reactive species absorbed onto the glass quickly at the growth temperature of ~ 580 °C, leading to the formation of a horizontal carbon buffer layer. With increasing growth time, the carbon atoms migrated on the buffer layer through the formation of small carbon nanosheets or carbon islands several-nanometers thick. With further increasing growth time, graphene nanosheets grew vertically and extended over the entire glass surface.

The preference of graphene to grow perpendicularly to rather than in parallel with the glass substrate can be explained as follows: i) Due to the different chemical bonding nature of the glass substrate and the graphitic carbon, a polycrystalline carbon buffer layer is usually formed to eliminate the interface strain effect, followed by the formation of many defects and curved areas [14]; ii) strain energy exists in the curved edges and defects for the initially deposited carbon layers, and a growth direction transition from parallel to vertical is favored to release the strain energy [21];

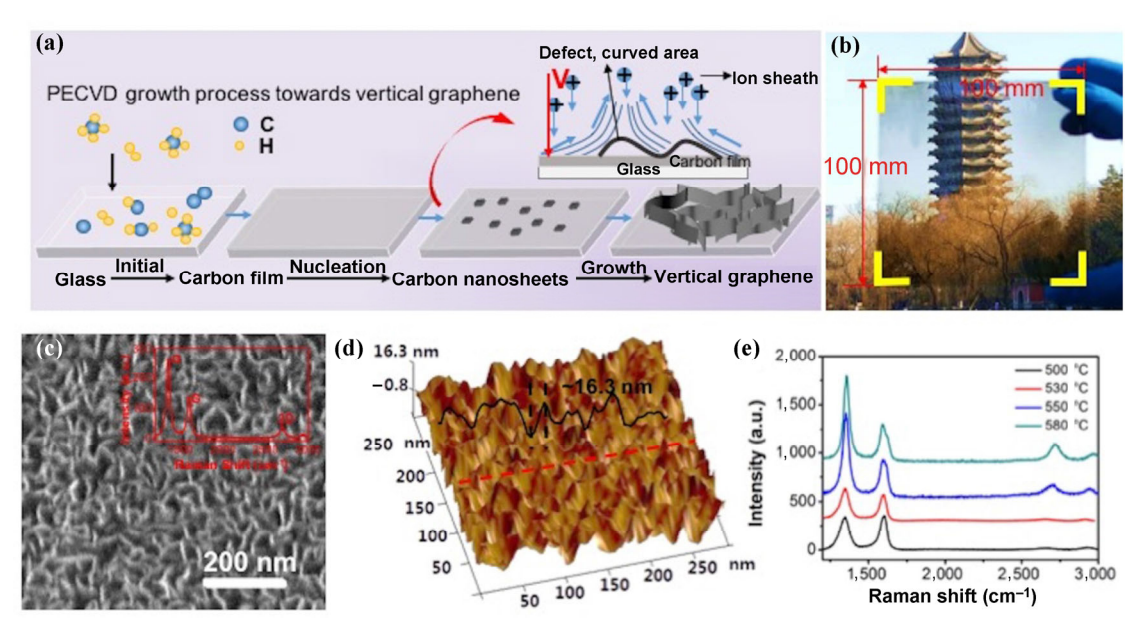


Figure 1 PECVD growth towards vertical graphene. (a) Schematic illustration of the direct growth of VG nanosheets on glass substrates by a dc-PECVD route. Inset: The sheath effect and ion bombardment between bulk plasma and defect/curved areas of the glass substrates. (b) Photograph of a 6-inch (along diagonal direction) white float glass substrate after PECVD growth at 580 °C for 8 min. (c) SEM image of the VG nanosheets grown on the glass at 580 °C for 10 min. Inset is a typical Raman spectrum of the synthesized graphene nanowalls. (d) Corresponding AFM image of the VG nanosheets. Inset shows the section view of the image along the red-dashed line direction. (e) Raman spectra of the VG grown directly on soda-lime glass by dc-PECVD at various substrate temperatures at 500, 530, 550, and 580 °C.

iii) the surface diffusion energy (~ 0.13 eV) of a carbon atom on the graphite surface is much lower than that of the absorption energy (~ 1.8 eV) [22], which could assist in the migration of carbon atoms along the graphene nanosheet surface, leading to the vertical growth behavior; iv) in the dc-PECVD system, the electric field in the plasma sheath is aligned vertically to the substrate surface, which can impart an overwhelming effect on the growth of the VG nanosheets [23–25].

A landscape is clearly demonstrated through the dc-PECVD growth of graphene on 10 cm × 10 cm soda-lime glass for 8 min at 580 °C (Fig. 1(b)). The graphene coated glass sample exhibits relatively high transparency and uniformity, as can be seen in the image in Fig. 1(b). The representative scanning electron microscopy (SEM) morphology in Fig. 1(c) confirms the existence of VG nanosheets, and the inserted Raman spectrum shows characteristic peaks at 1,353 cm⁻¹ (D band), 1,592 cm⁻¹ (G band), and 2,698 cm⁻¹ (2D band), similar to VG nanosheets synthesized on silicon substrates by mw-PECVD [26]. Figure S2 in the ESM

also provides detailed explanations of a representative Raman spectrum of the VG on glass. The vertical geometry was also confirmed in the 3D atomic force microscope (AFM) image (Fig. 1(d)) and its section view, showing a highly corrugated surface with a corrugation of ~ 16.3 nm.

The controllable growth of the VG nanosheets on glass with desirable characteristics is essential for its application in gas sensors, biosensors, and energy storage devices [10-14]. Previous studies have indicated that the structure and morphology of VG nanosheets are quite sensitive to the growth parameters, including substrate temperature, gas composition, carbon source, and growth time [27]. The effect of substrate and heating temperature on the quality of VG grown on glass is also shown in Fig. 1(e). From the results, a starting temperature of ~ 500 °C was established for the growth of high quality VG nanosheets on soda-lime glass without the aid of metal catalysts. For better sample quality, a critical temperature of ~ 580 °C was selected to avoid the melting of glass substrates in the PECVD growth process. Moreover, the type of carbon precursor and the ratio of CH₄:H₂ were found to have large effects on the quality of the VG on glass (Fig. S3 in the ESM).

For details of the unique 3D growth character, AFM images were taken of soda-lime glass at different dc-PECVD growth durations of 2, 6, and 15 min, and are presented in Figs. 2(a)–2(c), respectively, at a growth temperature of 580 °C (with additional images in Fig. S4 in the ESM). In the early growth stage (2 min), a polycrystalline carbon layer of ~ 1.4 nm in corrugation was formed on the glass surface (Fig. 2(a)). At 6 min, a single crystal nanosheet appeared on the carbon layer, with a perpendicular growth orientation to the glass surface. Totally covered VG nanosheets appeared between 8-10 min. This vertical growth behavior is proposed to be mediated by the concurrent effects from the vertical electric field, the fast diffusion of carbon atoms, and the strain energy at the curved edges. At 15 min, the surface corrugation of the VG nanosheets reached ~ 90.5 nm, which is larger than the corrugation values of 12.3, 16.3, and 35.8 nm, at 8, 10, and 13 min respectively. In this regard, the corrugation extent of the VG nanosheets can be precisely tailored by varying growth time. Moreover, with a similar transparency of 79%, an approximately 6 times faster growth rate was achieved on glass with the dc-PECVD method, compared to previously published work in which a rf-PECVD route was used [7]. The faster growth rate is likely mediated by the high density of reactive carbon radicals generated under the high voltage that was applied between the two parallel plates of the PECVD system.

A series of experimental examinations including Raman, contact angle, transmittance, and resistance were then performed on the above mentioned VG nanosheets on glass. Figure 2(d) clearly shows the increase in $I_{\rm 2D}/I_{\rm G}$ (from 0.11 to 0.74) with increasing growth time, indicating the improvement of crystal quality and domain size of the VG nanosheets. However, the D band is still significant at 8, 10, and

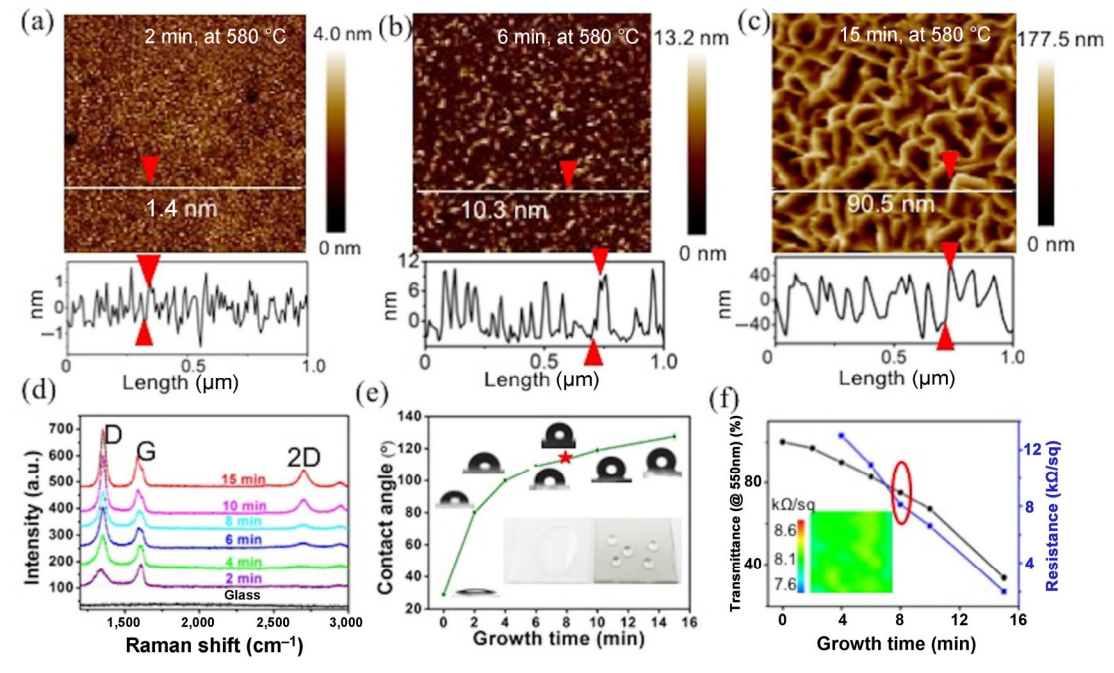


Figure 2 AFM images of directly grown VG nanosheets on soda-lime glass by a dc-PECVD route at various growth time. (a) 2 min, (b) 6 min, (c) 15 min growth time, while keeping other growth parameters constant (40 sccm CH_4 , 20 sccm H_2 , 580 °C). The corresponding height profiles are plotted along the lines shown in (a)–(c). The red arrows in each image mark the corrugation differences. (d) Raman spectra characterizations, (e) contact angles, (f) corresponding sheet resistances and UV–vis transmittance spectra at 550 nm for the VG nanosheets on glass at growth times of 2, 4, 6, 8, 10, and 15 min, respectively. The inset in (e) shows the hydrophobic and hydrophilic nature of the VG nanosheets on the glass sample with a transmittance of 75% at 550 nm (right) and bare glass surface (left). The inset in (f) shows the sheet resistance mapping of a 2 cm × 2 cm vertical graphene glass sample at growth time of 8 min.

15 min, which is likely a result of the concurrent effects of the vertical orientation, small domain size, and defects at the sharp edges. Water dropping displays were also performed on the as-grown VG nanosheets on glass experiencing growth time from 2 to 15 min, with pristine glass as a control (Fig. 2(e)). The photograph of the pristine glass and a sample at a growth time of 8 min (inset of Fig. 2(e), 2 cm × 2 cm in size) are also presented both before and after the water dropping tests. Notably, the surface wettability of the glass surface can be greatly modified by VG nanosheet coating. The contact angle (CA) was dramatically enlarged with increasing growth time of graphene. For the 2 min sample, owing to the formation of a carbon buffer layer, the CA became substantially larger-i.e., 80°-than the CA of the pristine glass with a contact angle of 27°. When graphene grows perpendicularly to the substrate gradually from 4, 6, 8, to 10 min, the wettability of the graphene glass changes along with the surface properties from hydrophilic to hydrophobic, with the CAs varying from 100°, 109°, 114°, to 120°, respectively. With prolonged growth time, the CA increased until it reached a maximum of 128° for 15 min sample. Such a gradually tunable hydrophobic surface property provides great promise for application in self-cleaning windows or water collecting devices.

Moreover, the transparency of the graphene glass at 550 nm can be precisely tuned with values of 97.0%, 90.0%, 82.9%, 75.2%, 67.1%, and 33.6% by varying growth time of graphene from 2, 4, 6, 8, 10 to 15 min, respectively, as shown in Fig. 2(f). The sheet resistance also varies significantly with values of ∞ , 13, 10.9, 8.1, 6.6, and 2 k Ω /square at 2, 4, 6, 8, 10, and 15 min, respectively. These results exemplify the tunability of the optical and electronic properties of the synthesized VG nanosheet-glass hybrid samples. Additionally, the conductivity of the graphene glass hybrid material is comparable to previously reported results at similar transmittance values for graphene nanowalls directly synthesized on glass substrates by rf- PECVD [7].

The VG nanosheet-glass hybrid material at a growth time of 8 min possesses a balanced performance between transmittance and sheet resistance of ~ 75.2% and 8.0 k Ω /square, respectively (Fig. 3(a)). To show the microscopic uniformity of the sample, the optical microscopy (OM) and corresponding Raman mapping of the G peak intensity were also obtained by transferring the as-grown graphene nanosheets from glass onto SiO₂/Si (Figs. 3(b) and 3(c)). The uniform

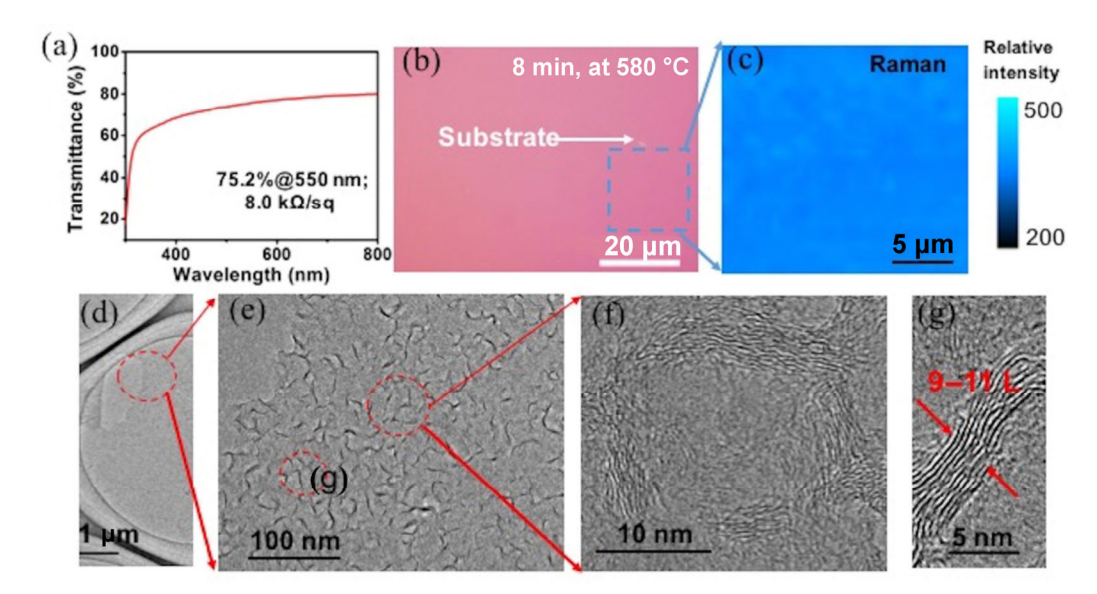


Figure 3 Characteristics of the microscopic structure and uniformity of the VG nanosheets at a growth time of 8 min (growth parameters: 40 sccm CH₄, 20 sccm H₂, 580 °C). (a) UV-vis transmittance spectrum of the VG nanosheet-glass with a sheet resistance of $\sim 8.0 \text{ k}\Omega/\text{square}$. (b) OM image of the VG nanosheets transferred onto a SiO₂/Si substrate. (c) Raman mapping showing the G peak intensity of the transferred sample on SiO₂/Si. (d)–(g) Sequential zoom-in TEM images of the VG nanosheets transferred onto copper grids.

color contrast in the OM image and Raman mapping demonstrate the excellent uniformity of the VG nanosheets. Moreover, transmission electron microscopy (TEM) characterizations were also performed on the transferred samples on TEM grids to view the thickness and the detailed structures, and are shown in sequential zoom-in images in Figs. 3(d)–3(g). It is clear that the graphene nanosheets consist of 9-11 graphene layers with an interlayer spacing of ~ 0.34 nm. An individual VG nanosheet usually possesses a lateral dimension of tens of nanometers and a thickness of only ~ 3.4 nm (Figs. 3(f) and 3(g)). In this regard, each graphene nanowall can be considered as a quasi-two-dimensional structure with strong anisotropy. Furthermore, X-ray photoelectron spectroscopy (XPS) was used to investigate the as-grown graphene glass at a growth time of 8 min and is shown in Fig. S5 in the ESM. The absence of signal arising from any metallic elements is evidence of the catalyst-free growth mechanism, as well as the good crystal quality of the dc-PECVDderived graphene on the glass substrates.

Taking advantage of their unique structure and intrinsic properties, the VG nanosheet-glass hybrid materials were then utilized for collecting solar energy and converting it into heat, leading to the increase in the surface temperature of the glass. Considering the good transparency and low-cost of the material, as well as its amenability to large-scale production, this novel hybrid material should have great potential in the fabrication of a new kind of photothermal device. To validate the probability of its use for such a device, further experiments were performed to test its thermal energy conversion. Figures 4(a) and 4(b) show schematic illustrations of the solar-thermal conversion difference between normal soda-lime glass and VG nanosheets on the glass. For the actual experiments, a series of VG glass hybrid samples with different transparencies were exposed to solar simulation, with the pristine glass as a control. The light source used in the experiments was a solar simulator (SAN-EIELECTRIC XES-160S1) with a lamp irradiation power maintained at 1 kW/m².

As reported previously, through designing appropriate geometries of metallic nanoshells, the photothermal conversion of the full solar spectrum can be achieved using the antireflective and light trapping properties

of such metallic nanostructures [28]. Unlike insulating glass and other metallic-based materials, graphene has broad absorption due to its intrinsic Dirac cone band structure [1, 2].

The intriguing 3D corrugated structure of the VG nanosheets (Fig. S6 in the ESM) enhance the sunlight adsorption and the induced heating effect (Fig. S7 in the ESM). In this regard, VG nanosheets can be considered as a kind of anti-reflective coating layer [29], providing an "optical trap". The light irradiation in the inner valley regions of VG nanosheets undergoes multiple internal reflections, as schematically illustrated in Fig. 4(c) and Fig. S7 in the ESM. The light adsorption ratio can be enhanced by increasing the collision probability between photons and the surface of the nanosheets.

With increasing surface corrugation of the VG nanosheets (by extending the dc-PECVD growth time), the length and height of nanosheets as a "light trap" are increased while the transmittance decreased. Accordingly, the reflectance of the VG nanosheetglass decreases dramatically (Fig. 4(d)). A low reflectance usually implies enhanced light trapping and absorption in the VG nanosheet-glass. In this study, the unique VG structure exhibits a porous morphology that possesses sub-wavelength absorption. When incident light is transmitted into the VG nanosheet region, scattering and internal reflections occur within the VG nanosheets, resulting in the enhancement of light trapping, similar to that of silicon-nanowires [30]. Without deliberate design of the detailed nanostructures, just by tailoring the surface corrugation or varying growth time, efficient full solar spectrum light-to-heat conversion can be attained.

Under the irradiation of the solar simulator, the temperature of pristine glass rises from room temperature (~ 25 °C) to 36.39 ± 0.15 °C. In contrast, the VG glass hybrid reached a much higher temperature of 58.41 ± 1.59 °C at a transmittance of 34% at 550 nm. From the contour maps of surface temperature obtained by infrared imaging systems (Fig. 4(e)), the temperature differences among different VG nanosheet-glass hybrids are clear, with temperatures of 42.23 ± 0.77 , 47.18 ± 1.18 , 48.43 ± 1.95 , and 58.41 ± 1.59 °C, with transmittances of 97%, 83%, 75%, and 34%, respectively. Moreover, the uniform color contrast and corresponding histogram

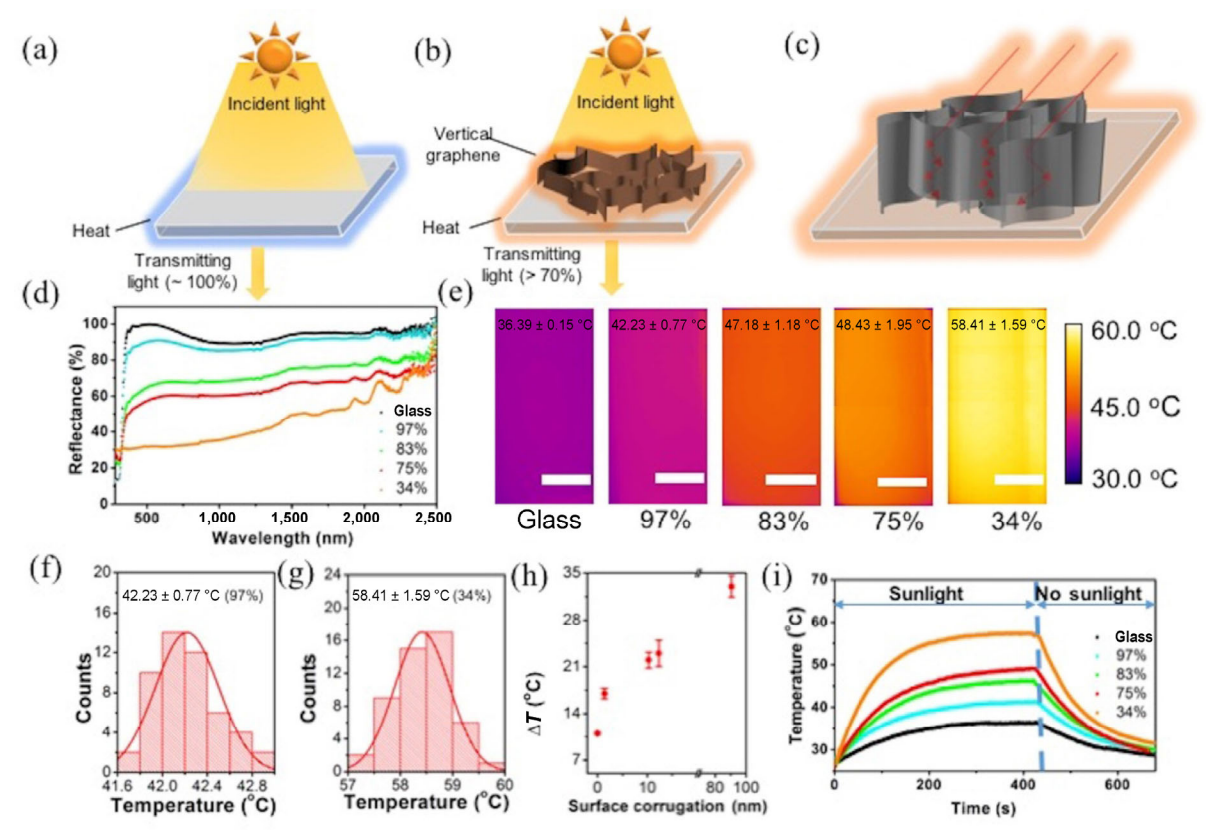


Figure 4 Photothermal applications of VG nanosheet-glass. (a) and (b) Schematic illustrations of glass and VG nanosheets-glass based photothermal devices. (c) Schematic illustration of the internal light reflection through graphene nanowalls synthesized on glass by a dc-PECVD route. (d) Reflectance spectra in the wavelength range of 300–2,500 nm for VG nanosheets-glass synthesized at various growth time (0, 2, 6, 8, and 15 min). (e) Infrared thermal imaging camera photographs of the bare glass surfaces (1 cm × 2 cm), and VG nanosheets glass hybrid samples, respectively, under the irradiation of simulation sunlight. Scale bar: 5 mm. (f) and (g) Corresponding surface temperature histogram statistics of the two samples with the transmittances of 97% and 34% @550 nm, respectively. (h) Curve for the surface temperature increase versus surface corrugation of vertically aligned graphene glass. (i) Temperature versus time curves of pristine glass and vertically oriented graphene/glass hybrids under the irradiation of simulated solar source, respectively.

statistics for the surface temperature of the samples (with transmittances of 97% and 34% in Figs. 4(f) and 4(g), respectively) indicate the uniform heating effect on the VG nanosheet-glass substrates (more results can be seen in Fig. S8 in the ESM).

Figure 4(h) shows the surface temperature increase of the VG glass samples with different surface corrugation. By increasing the surface corrugation of the VG nanosheets, the light-to-heat conversion efficiency is improved. In addition, the surface temperature versus irradiation time curves of the pristine glass and the VG nanosheets-glass samples are shown in Fig. 4(i). Clearly, the surface temperature of the different samples gradually increases and reaches a maximum value at similar exposure time (~ 7 min). As

can be seen in Fig. S9 in the ESM, it can be concluded that the saturation time for the surface temperature of the various samples is mainly related to the size of the samples rather than the corrugation of VG nanosheets. After removing the light source, the surface temperature of the samples dropped gradually within 3–5 min, but remained slightly above room temperature. To sum up, VG on glass has exhibited a remarkable photothermal property, which should shed light on its practical applications, e.g., in transparent heating windows and warmth solar-accumulated devices. Further, the possibility of batch production in the case of the dc-PECVD for achieving large-scale, highly uniform hybrid materials should make this perspective become more realistic.

A 6-inch uniform VG glass hybrid (as shown in Fig. 5(a)) was then used to fabricate a large-scale photothermal device. The hybrid presented a transmittance of 70% at 550 nm. The corresponding 2D and 3D AFM images (Fig. 5(b)) confirm the vertically oriented morphology and the surface corrugation ~ 11.6 nm of the VG nanosheets grown on the soda-lime glass. Raman spectra (Fig. 5(c)) of the VG nanosheetglass sample collected from the positions shown in Fig. 5(a) indicate the large-scale uniformity of the graphene sample. As a solarthermal device, the sample was exposed directly under the simulated solar source without special treatment. A uniform infrared thermal imaging camera photograph of the 6-inch VG glass was obtained and shown in Fig. 5(d). The surface temperature was found to increase from room temperature (~ 25 °C) to 49.58 ± 2.42 °C. The histogram statistics of the surface temperature and surface temperature versus time curve are displayed in Fig. S7 in the ESM. As can be seen in the large-scale uniform mapping photograph in Fig. 5(d), uniform heating of the VG nanosheet-glass hybrid under the simulated solar source irradiation can be achieved with the dc-PECVD-derived VG soda-lime glass.

In conclusion, we have developed a dc-PECVD route to grow VG directly on 6-inch soda-lime glass without introduction of metal catalyst, with a synthesis temperature below the softening point of normal glass. We also found that the morphology, surface hydrophobicity, optical transparency, and conductivity can be precisely tuned by adjusting the growth parameters, especially the growth time of graphene. The highly corrugated nature of VG nanosheets makes them suitable candidates for high performance photothermal applications. The surface temperature of graphene glass at 75% transmittance was higher by 15 °C than that of the pristine glass. This study is the first experimental demonstration of the direct application of a VG glass hybrid material for scalable and practical use in a photothermal device, and should spur its applications in related fields.

Acknowledgements

This work was financially supported by the National Key Research and Development Program of China

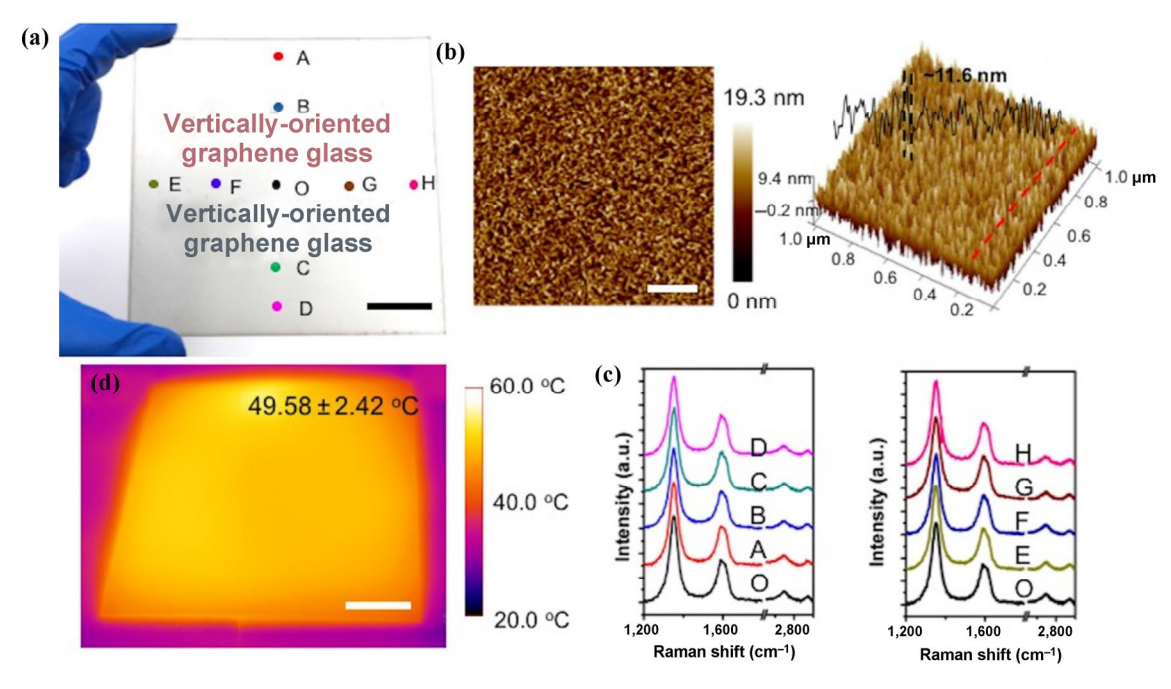


Figure 5 6-inch uniform VG glass for solarthermal applications. (a) Photograph of a 6-inch (along the diagonal direction) uniform graphene glass (PECVD growth at 580 °C for 8 min 30 s, 40 sccm CH_4 , 20 sccm H_2 with a transmittance of \sim 70% at 550 nm). (b) Corresponding 2D and 3D AFM images of the morphology of the VG nanosheet-glass. Inset shows the section view of the image along the red-dashed line. (c) Raman spectra of the as-grown VG on soda-lime glass, with the selected points exemplifying typical regions of the surface. (d) Infrared thermal imaging camera photograph of a 6-inch VG nanosheet-glass. Scale bar: 20 mm for (a) and (d), 200 nm for (b).

(No. 2016YFA0200103), the Beijing Municipal Science and Technology Commission (No. Z161100002116020), the Ministry of Science and Technology of China (No. 2013CB932603), the National Natural Science Foundation of China (Nos. 51432002, 51290272 and 51472008), the Beijing Municipal Science and Technology Planning Project (No. Z151100003315013), and the Certificate of China Postdoctoral Science Foundation Grant (No. 2016M590010).

Electronic Supplementary Material: Supplementary material (detailed experimental section, schematic of the fabrication process, Raman spectroscopy measurements, AFM imaging and so on) is available in the online version of this article at https://doi.org/10.1007/s12274-017-1839-1.

References

- [1] Novoselov, K. S.; Geim, A. K.; Morozov, S. V.; Jiang, D.; Zhang, Y.; Dubonos, S. V.; Grigorieva, I. V.; Firsov, A. A. Electric field effect in atomically thin carbon films. *Science* 2004, 306, 666–669.
- [2] Novoselov, K. S.; Geim, A. K.; Morozov, S. V.; Jiang, D.; Katsnelson, M. I.; Grigorieva, I. V.; Dubonos, S. V.; Firsov, A. A. Two-dimensional gas of massless Dirac fermions in graphene. *Nature* 2005, 438, 197–200.
- [3] Geim, A. K.; Novoselov, K. S. The rise of graphene. *Nat. Mater.* **2007**, *6*, 183–191.
- [4] Novoselov, K. S.; Fal'ko, V. I.; Colombo, L.; Gellert, P. R.; Schwab, M. G.; Kim, K. A roadmap for graphene. *Nature* 2012, 490, 192–200.
- [5] Sun, J. Y.; Chen, Y. B.; Priydarshi, M. K.; Chen, Z.; Bachmatiuk, A.; Zou, Z. Y.; Chen, Z. L.; Song, X. J.; Gao, Y. F.; Rümmeli, M. H. et al. Direct chemical vapor deposition-derived graphene glasses targeting wide ranged applications. *Nano Lett.* 2015, 15, 5846–5854.
- [6] Chen, Y. B.; Sun, J. Y.; Gao, J. F.; Du, F.; Han, Q.; Nie, Y. F.; Chen, Z. L.; Bachmatiuk, A.; Priydarshi, M. K.; Ma, D. L. et al. Growing uniform graphene disks and films on molten glass for heating devices and cell culture. *Adv. Mater.* 2015, 27, 7839–7846.
- [7] Sun, J. Y.; Chen, Y. B.; Cai, X.; Ma, B. J.; Chen, Z. L.; Priydarshi, M. K.; Chen, K.; Gao, T.; Song, X. J.; Ji, Q. Q. et al. Direct low-temperature synthesis of graphene on various glasses by plasma-enhanced chemical vapor deposition for versatile, cost-effective electrodes. *Nano Res.* 2015, 8, 3496–3504.

- [8] Sun, J. Y.; Chen, Z. L.; Yuan, L.; Chen, Y. B.; Ning, J.; Liu, S. W.; Ma, D. L.; Song, X. J.; Priydarshi, M. K.; Bachmatiuk, A. et al. Direct chemical-vapor-deposition-fabricated, large-scale graphene glass with high carrier mobility and uniformity for touch panel applications. ACS Nano 2016, 10, 11136–11144.
- [9] Chen, X. D.; Chen, Z. L.; Jiang, W. S.; Zhang, C. H.; Sun, J. Y.; Wang, H. H.; Xin, W.; Lin, L.; Priydarshi, M. K.; Yang, H. et al. Fast growth and broad applications of 25-inch uniform graphene glass. *Adv. Mater.* 2017, 29, 1603428.
- [10] Miller, J. R.; Outlaw, R. A.; Holloway, B. C. Graphene double-layer capacitor with ac line-filtering performance. *Science* **2010**, *329*, 1637–1639.
- [11] Yu, K. H.; Bo, Z.; Lu, G. H.; Mao, S.; Cui, S. M.; Zhu, Y. W.; Chen, X. Q.; Ruoff, R. S.; Chen, J. H. Growth of carbon nanowalls at atmospheric pressure for one-step gas sensor fabrication. *Nanoscale Res. Lett.* 2011, 6, 202.
- [12] Soin, N.; Roy, S. S.; Lim, T. H.; McLaughlin, J. A. D. Microstructural and electrochemical properties of vertically aligned few layered graphene (FLG) nanoflakes and their application in methanol oxidation. *Mater. Chem. Phys.* 2011, 129, 1051–1057.
- [13] Shang, N. G.; Papakonstantinou, P.; McMullan, M.; Chu, M.; Stamboulis, A.; Potenza, A.; Dhesi, S. S.; Marchetto, H. Catalyst-free efficient growth, orientation and biosensing properties of multilayer graphene nanoflake films with sharp edge planes. Adv. Funct. Mater. 2008, 18, 3506–3514.
- [14] Yang, C. Y.; Bi, H.; Wan, D. Y.; Huang, F. Q.; Xie, X. M.; Jiang, M. H. Direct PECVD growth of vertically erected graphene walls on dielectric substrates as excellent multifunctional electrodes. *J. Mater. Chem. A* 2013, 1, 770–775.
- [15] Wu, Y.; Qiao, P.; Chong, T.; Shen, Z. Carbon nanowalls grown by microwave plasma enhanced chemical vapor deposition. *Adv. Mater.* **2002**, *14*, 64–67.
- [16] Wang, J. J.; Zhu, M. Y.; Outlaw, R. A.; Zhao, X.; Manos, D. M.; Holloway, B. C. Synthesis of carbon nanosheets by inductively coupled radio-frequency plasma enhanced chemical vapor deposition. *Carbon* 2004, 42, 2867–2872.
- [17] Liu, W. H.; Dang, T.; Xiao, Z. H.; Li, X.; Zhu, C. C.; Wang, X. L. Carbon nanosheets with catalyst-induced wrinkles formed by plasma-enhanced chemical-vapor deposition. *Carbon* 2011, 49, 884–889.
- [18] Ma, Y. F.; Jang, H.; Kim, S. J.; Pang, C.; Chae, H. Copperassisted direct growth of vertical graphene nanosheets on glass substrates by low-temperature plasma-enhanced chemical vapour deposition process. *Nanoscale Res. Lett.* 2015, 10, 308.
- [19] Bo, Z.; Yu, K. H.; Lu, G. H.; Wang, P. X.; Mao, S.; Chen, J. H. Understanding growth of carbon nanowalls at atmospheric pressure using normal glow discharge plasma-enhanced chemical vapor deposition. *Carbon* 2011, 49, 1849–1858.

- [20] Obraztsov, A. N.; Zolotukhin, A. A.; Ustinov, A. O.; Volkov, A. P.; Svirko, Y.; Jefimovs, K. DC discharge plasma studies for nanostructured carbon CVD. *Diamond Relat. Mater.* 2003, 12, 917–920.
- [21] Zhao, J.; Shaygan, M.; Eckert, J.; Meyyappan, M.; Rummeli, M. H. A growth mechanism for free-standing vertical graphene. *Nano Lett.* 2014, 14, 3064–3071.
- [22] Louchev, O. A.; Sato, Y.; Kanda, H. Growth mechanism of carbon nanotube forests by chemical vapor deposition. *Appl. Phys. Lett.* 2002, 80, 2752–2754.
- [23] Wu, Y. H.; Yang, B. J. Effects of localized electric field on the growth of carbon nanowalls. *Nano Lett.* **2002**, *2*, 355–359.
- [24] Wu, Y. H.; Yang, B. J.; Zong, B. Y.; Sun, H.; Shen, Z. X.; Feng, Y. P. Carbon nanowalls and related materials. *J. Mater. Chem.* 2004, 14, 469–477.
- [25] Zhu, M. Y.; Wang, J. J.; Holloway, B. C.; Outlaw, R. A.; Zhao, X.; Hou, K.; Shutthanandan, V.; Manos, D. M. A mechanism for carbon nanosheet formation. *Carbon* 2007, 45, 2229–2234.

- [26] Ni, Z. H.; Fan, H. M.; Feng, Y. P.; Shen, Z. X.; Yang, B. J.; Wu, Y. H. Raman spectroscopic investigation of carbon nanowalls. J. Chem. Phys. 2006, 124, 204703.
- [27] Bo, Z.; Yang, Y.; Chen, J. H.; Yu, K. H.; Yan, J. H.; Cen, K. F. Plasma-enhanced chemical vapor deposition synthesis of vertically oriented graphene nanosheets. *Nanoscale* 2013, 5, 5180–5204.
- [28] Bae, K.; Kang, G. M.; Cho, S. K.; Park, W.; Kim, K.; Padilla, W. J. Flexible thin-film black gold membranes with ultrabroadband plasmonic nanofocusing for efficient solar vapour generation. *Nat. Commun.* 2015, 6, 10103.
- [29] Raut, H. K.; Ganesh, V. A.; Nair, A. S.; Ramakrishna, S. Anti-reflective coatings: A critical, in-depth review. *Energy Environ. Sci.* 2011, 4, 3779–3804.
- [30] Hoch, L. B.; O'Brien, P. G.; Jelle, A.; Sandhel, A.; Perovic, D. D.; Mims, C. A.; Ozin, G. A. Nanostructured indium oxide coated silicon nanowire arrays: A hybrid photothermal/ photochemical approach to solar fuels. ACS Nano 2016, 10, 9017–9025.